УДК: 622.276.4; 622.276.6; 622.279.4; https://doi.org/10.37878/2708-0080/2024-1.14
https://orcid.org/0009-0007-5726-7899
https://orcid.org/0000-0001-9372-7345
https://orcid.org/0000-0002-9820-7952
https://orcid.org/0000-0002-8137-4535
https://orcid.org/0000-0003-0781-2434
https://orcid.org/0000-0002-6009-9730

THE EFFECT OF POLYMER GEL ON THE OIL AND WATER PERMEABILITY DAMAGE IN A MICROFLUIDIC DEVICE

ZH. KULI[1],
master of technical sciences,
doctoral student,
kuliev.zhanserik@gmail.com

SH. KENZHEKHANOV[2],
PhD,
sh.kenzhekhan@gmail.com

I. GUSSENOV[1],
PhD,
iskander.gussenov@gmail.com

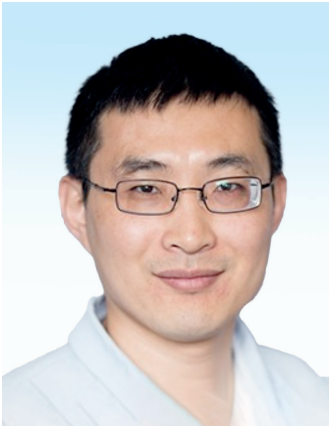

X. YIN[3,4],
PhD,
xyin@eitech.edu.cn

N. TILEUBERDI[5],
PhD,
1983nureke@gmail.com

M. MASHRAPOVA[5],
PhD,
moldir_m_m@mail.ru

[1]SATBAYEV UNIVERSITY
22/5, Satpayev str., Almaty, 050000, Republic of Kazakhstan

[2]JSC «PHYSTECH II»
Microdistrict 4, building 73, Mangystau Region, Aktau, 130000, Republic of Kazakhstan

[3]EASTERN INSTITUTE OF TECHNOLOGY, NINGBO
568 Tongxin Road, Zhenhai District, Ningbo, Zhejiang, China

[4]COLORADO SCHOOL OF MINES
1500 Illinois St, Golden, CO 80401, USA

[5]INSTITUTE OF GEOLOGICAL SCIENCES NAMED AFTER K.I. SATPAEV
Valikhanov Street, 69/94, Qabanbay Batyr Street, Almaty, 050010, Republic of Kazakhstan

Microfluidics, a rapidly advancing field, finds wide applications in various domains, including enhanced oil recovery. This study delineates the methodology for fabricating a microchip with channels having a width of 50 μm, designed to simulate and visualize fluid flow in porous media. The microfluidic device was constructed using NOA81, a UV-curable polymer. Upon curing, it forms a robust and transparent microchip structure suitable for precise fluid control and analysis in microfluidic applications. Flood experiments conducted on the microchip revealed that the introduction of a 0.5 wt% polymer gel into the model's channels resulted in a reduction of water permeability by a factor of 106 and 25 at the shock front and after injection pressure stabilized, respectively. In contrast, oil permeability was reduced by at least 40 times.

KEYWORDS: *microfluidics, microchip, oil permeability, polymer gel, enhanced oil recovery.*

МИКРОМОДЕЛЬДІҢ МҰНАЙ МЕН СУДЫ ӨТКІЗГІШТІГІНЕ ПОЛИМЕР ГЕЛЫНІҢ ӘСЕРІ

Ж. ҚҰЛИ[1], техника ғылымдарының магистрі, докторант, *kuliev.zhanserik@gmail.com*
Ш. КЕНЖЕХАНОВ[2], PhD, *sh.kenzhekhan@gmail.com*
И. ГУСЕНОВ[1], PhD, *iskander.gussenov@gmail.com*
К. ИНЬ[3,4], PhD, *xyin@eitech.edu.cn*
Н.ТІЛЕУБЕРДІ[5], PhD, *1983nureke@gmail.com*
М.А. МАШРАПОВА[5], PhD, *moldir_m_m@mail.ru*

[1]SATBAYEV UNIVERSITY
Сәтбаев к., 22, 050013, Алматы қ, Қазақстан Республикасы,

[2]АО «PHYSTECH II»
Ақтау қ., 4 ықшам ауданы, 73 ғимарат, 130000, Маңғыстау обл., Қазақстан Республикасы

[3]EASTERN INSTITUTE OF TECHNOLOGY, NINGBO
568 Tongxin Road, Zhenhai District, Ningbo, Zhejiang, China

[4]COLORADO SCHOOL OF MINES
1500 Illinois St, Golden, CO 80401, USA

[5]Қ.И. СӘТБАЕВ АТЫНДАҒЫ ГЕОЛОГИЯЛЫҚ ҒЫЛЫМДАР ИНСТИТУТЫ
Қабанбай батыр к., 69, 050010, Алматы қ., Қазақстан Республикасы

Микрофлюидика – бұл әртүрлі салаларда, соның ішінде мұнай алуды арттыруда кеңінен қолданылатын қарқынды дамып келе жатқан сала. Бұл зерттеу кеуекті ортадағы сұйық ағынын модельдеуге және визуализациялауға арналған ені 50 мкм арналары бар микрочипті жасау әдістемесін сипаттайды. Микрофлюидтік құрылғы сұйық шыны негізгі субстрат материалы ретінде қызмет ететін золь-гель процесін қолдана отырып жасалған. Бұл тәсіл сұйық шынының бірегей қасиеттерін пайдаланады, ол қатайған кезде микрофлюидті қолданғанда сұйықтықты дәл бақылау және талдау үшін өте қолайлы берік және мөлдір микромодель құрылымын құрайды. Микрофлюидті чип – микро деңгейде сүзу процестерін визуализациялауға жарамды, берік және мөлдір құрылымды құрай отырып, ультракүлгін сәулемен жарықтану кезінде қатып қалатын NOA81 көмегімен жасалатын полимер. Сүзу тәжірибелері көрсеткендей, концентрациясы 0,5 салмақ.% гель-полимерлі кешенді модель арналарында су бойынша өткізгіштігінің 106 есе максималды төмендеуіне әкелді және қысым тұрақтанғаннан кейін 25 есе азайды. Мұнай бойынша өткізгіштігі кем дегенде 40 есе төмендеді.

ТҮЙІН СӨЗДЕР: *микрофлюид, микрочип, мұнайөткізгіштік, полимерлі гель, мұнай бергіштіктің артуы.*

ВЛИЯНИЕ ПОЛИМЕРНОГО ГЕЛЯ НА ПРОНИЦАЕМОСТЬ МИКРОМОДЕЛИ ПО НЕФТИ И ВОДЕ

Ж. ҚҰЛИ[1], магистр технических наук, докторант, *kuliev.zhanserik@gmail.com*
Ш. КЕНЖЕХАНОВ[2], PhD, *sh.kenzhekhan@gmail.com*
И. ГУСЕНОВ[1], PhD, *iskander.gussenov@gmail.com*
К. ИНЬ[3,4], PhD, *xyin@eitech.edu.cn*
Н.ТІЛЕУБЕРДІ[5], PhD, *1983nureke@gmail.com*
М.А. МАШРАПОВА[5], PhD, *moldir_m_m@mail.ru*

[1]SATBAYEV UNIVERSITY
Республика Казахстан, 050013, г. Алматы, ул. Сатпаева, 22

[2]АО «PHYSTECH II»
Республика Казахстан, 130000, Мангистауская обл., г. Актау, микрорайон 4, здание 73

[3]EASTERN INSTITUTE OF TECHNOLOGY, NINGBO
568 Tongxin Road, Zhenhai District, Ningbo, Zhejiang, China

[4]COLORADO SCHOOL OF MINES
1500 Illinois St, Golden, CO 80401, USA

[5]ИНСТИТУТ ГЕОЛОГИЧЕСКИХ НАУК ИМЕНИ К. И. САТПАЕВА
Республика Казахстан, 050010, г. Алматы, уг. ул. Валиханова, 69/94, Қабанбай батыра

Микрофлюидика – быстро развивающаяся область, широко применяемая в различных областях, включая повышение нефтеотдачи пластов. В этом исследовании описывается методология изготовления микрочипа с каналами шириной 50 мкм, предназначенного для моделирования и визуализации потока жидкости в пористых средах. Микрофлюидный чип был изготовлен с использованием NOA81 – полимер, который затвердевает при облучении ультрафиолетовым светом, образуя прочную и прозрачную структуру, подходящую для визуализации фильтрационных процессов на микроуровне. Фильтрационные эксперименты показали, что закачка гелеполимерной композиции с концентрацией 0,5

вес.% в каналы модели привела к максимальному уменьшению проницаемости по воде в 106 раз, и в 25 раз после стабилизации давления нагнетания. Проницаемость по нефти была снижена по крайней мере в 40 раз.

КЛЮЧЕВЫЕ СЛОВА: *микрофлюидика, микромодель, проницаемость по нефти, полимерный гель, увеличение добычи нефти.*

Introduction. Microfluidics enables the manipulation and processing of tiny fluid volumes, typically within the range of 10^{-9} to 10^{-18} L [1, 2]. This feat is accomplished through the intricate design of channels, with dimensions typically spanning from tens to hundreds of micrometres [3, 4]. The inherent versatility of microfluidic technology has led to its adoption in various industries, including medical diagnostics and the oil and gas sector, demonstrating its significant utility and adaptability.

Microfluidics serves as a valuable research area within Enhanced Oil Recovery (EOR), enabling the examination of fluid flow behaviors within the pores [5-7]. For example, by conducting microfluidic experiments utilizing glass micromodels, the authors of [8, 9] demonstrated the effect of wettability, crude oil composition, flooding mechanisms, and brine salinity on the recovery of oil. Of note, is that flooding procedures involving surfactants manifested superior effectiveness compared to regular water flooding.

Furthermore, the authors of [10] explored the application of silicon dioxide (SiO2) nanoparticles in suspension, with concentrations ranging from 0.1 to 2 wt%, to amplify oil recovery in a porous medium emulated through a microfluidic chip. The outcomes of this research show a direct correlation between nanoparticle concentration and the efficiency of oil recovery, with a remarkable enhancement of 16% observed at a nanoparticle concentration of 0.5 wt%.

Additionally, microfluidics was used for the visualization of oil flow through porous media filled with gel. The primary mechanism for oil permeability increase involves oil initially moving through the centers of pores, leading to displacement of some gel. As oil flooding continues, pathways in the pores broaden and multiply, with the gel dehydrating due to oil phase pressure [11].

In this study, microfluidic chips were used to observe the blockage of microchannels by polymer gels and to quantify the decrease in permeability for water and oil. The findings from this research can inform the design of gel treatments and support further investigations.

Materials and methods

Fluids

A 75 g/L NaCl solution prepared with water was used to saturate the model. The same fluid was used for preparation of the polymer solution, as well as the pre- and post-flush injections, i.e., brine injections before and after gel treatment.

A gas-free light crude oil (38° API) was used in the experiment.

The polymer solution contained 0.5 wt% of very-high-molecular-weight and 5%-hydrolysis-degree hydrolyzed polyacrylamide (HPAM). Gellation was triggered by 0.05 wt% of chromium (III) acetate hydroxide.

Materials used to fabricate the microchip

Poly(dimethylsiloxane) (PDMS).

Novel polymer Norland Optical Adhesive NOA81 produced by Norland Products Inc.
Silicon wafer with microchip layout.

Methodology of microchip fabrication and characterization

The fabrication of the microchip involves the following main steps:

1. Design the layout of the microchip in AutoCAD software.
2. Print the layout of the microchip on an emulsion mask.
4. Apply photoresist (KMPR1010, Kayaku AM) coating to the surface of a wafer.
5. UV-etch the layout of the microchip on the photoresist using the mask.
6. Develop the photoresist in a developer (AZ-300, Microchemicals).
7. Etch the silicon wafer.
8. Measure the depths of the channels in the produced silicon microchip using a Dektak IIA profilometer.
9. Transfer the pattern of the microchip from silicon to PDMS polymer using replica molding.
10. Transfer the pattern of the microchip from PDMS to NOA81 using replica molding, and then expose NOA81 to UV light for 1 min 20 sec for partial curing.
11. Cover the partially cured microchip pattern in NOA81 with a thin layer of partially cured NOA81 prepared on a cover glass. Then, expose the fully enclosed microchip pattern to UV light for the complete and final curing of the adhesive (1 minute duration).

All the steps listed above to produce microchips are shown in more detail in *Figure 1* and *Figure 2*.

Measurements by the profilometer showed that within the pattern the depths of the channels in the silicon microchip are 11-12 μm, whereas the depths of the inlet and outlet channels are 20-23 μm. The widths of the channels are 50 μm.

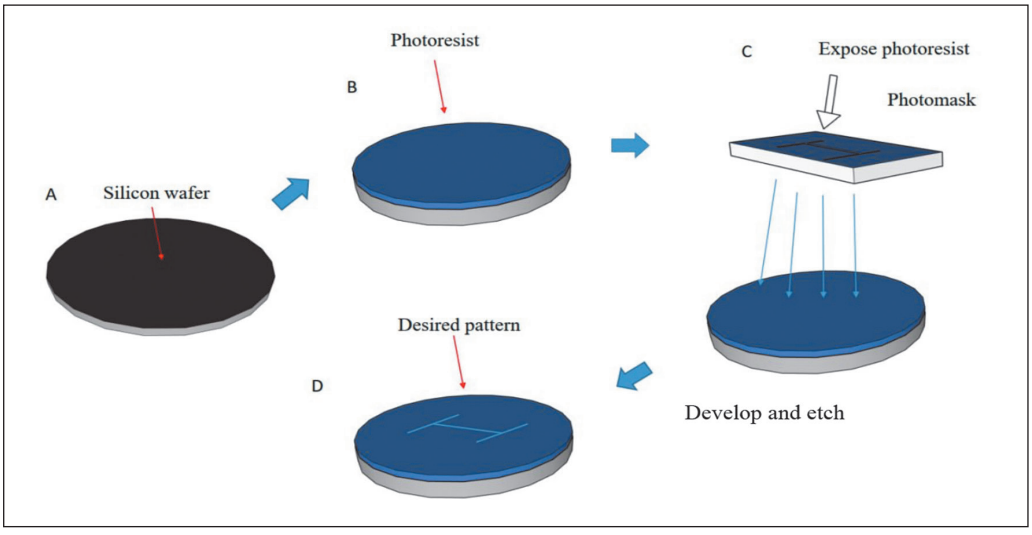

Figure 1 – **Steps of silicon microchip fabrication**
a) Preparation of the silicon wafer including surface cleansing and conditioning; b) Application of a photoresist coating onto the surface of the silicon wafer; c) Photolithographic exposure of the silicon wafer coated with photoresist material using a precision photomask; d) Pattern development and etching following photolithographic exposure

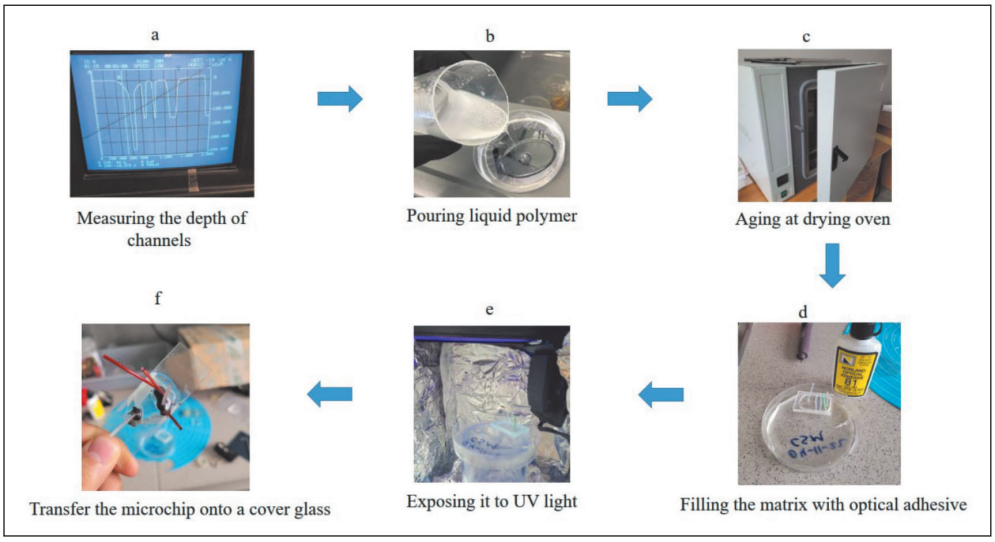

Figure 2 – **Steps of fabrication of NOA microchip**
a) measuring the depths of the channels on the silicon microchip; b) pouring liquid PDMS polymer onto the silicon microchip; c) solidification of PDMS in an oven; d) NOA molding over the PDMS; e) partial curing of the NOA microchip; f) coat and partially cure a thin layer of NOA on a cover glass, and cover the NOA microchip with the cover glass and then fully cure the NOA

Figure 3 shows a photo of an NOA micromodel saturated with brine. The photo was taken using a Levenhuk D320L Base 2-Microscope with a 3-megapixel resolution digital camera. For visual clarity, brine was dyed to enhance its detectability. By using dyed brine, we were able to differentiate the brine from injected oil and gel and visually measure their respective quantities.

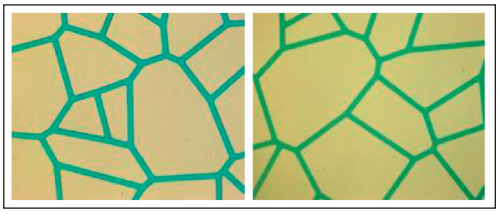

Figure 3 – **Brine saturated NOA microchip. Chanel size – 50 μm**

Methodology of conducting a flooding experiment on an NOA microchip

A flooding experiment consisted of the following steps:

1-Reduce the amount of air present in the microchip using a syringe.

2-Inject brine to fully saturate the microchip.

3-Inject oil in two steps:

Step 1 – Inject oil at room temperature overnight to ensure irreducible saturation of brine is established in the channels of the microchip.

Step 2 – Inject oil at 40 °C until the injection pressure stabilizes. 40 °C was chosen, reflecting the typical temperature in the oil fields of interest.

4-Pre-flush with brine: Inject brine at 40 °C to measure the injection pressure of the brine at oil's residual saturation.

5-Mix polymer solution with the gelling agent at room temperature, and then inject the solution into the microchip. Although the required temperature condition of the experiment is 40 °C, to avoid rapid gelation and the associated viscosity increase during the injection, we conducted this step at room temperature. Usually, it takes several hours for the solution to gel at 40 °C.

6-Age the microchip at 40 °C for 24 hr. This period allows gel to consistently develop in the microchip, gaining desired strength. In practice, gel always needs time to develop so that it becomes an effective barrier or plugging agent in the pores.

7-Post-flush with brine: Inject brine following the gel treatment to measure the residual resistance factor (RRF) to brine. Residual resistance factor is defined as the ratio between brine's permeability prior to gel injection and that after gel injection. It describes the reduction in brine's permeability due to gel plugging.

8-Inject oil (oil post-flush) to measure, after gel plugging and brine post-flush, the residual resistance factor to oil.

Results and Discussion

First, the viscosity of the polymer solution was measured using a rotational viscometer. Figure 4 shows that, at room temperature (18.3 °C) and a low angular velocity of 6 rotations per minute (RPM), the polymer solution has a relatively high viscosity of 156 cp. Gelation of the polymer solution significantly reduced its ability to flow. *Figure 5* illustrates the strengths of the gels after aging the solutions at room temperature and at 40 °C for 24 hours. Higher aging temperature resulted in increased gel strength.

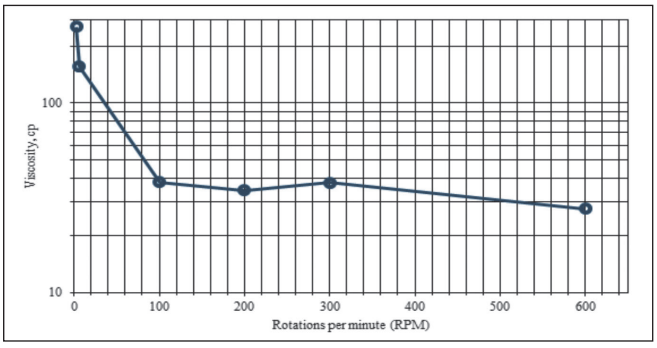

Figure 4 – **Viscosity of 0.5% very high molecular weight HPAM in 75 g/L NaCl brine at 18.3 °C**

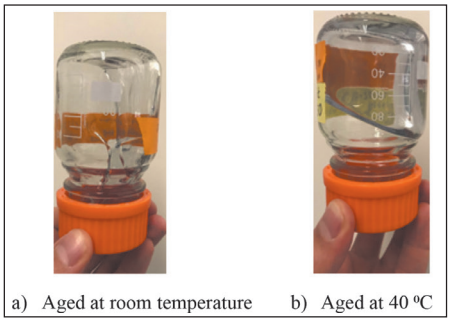

Figure 5 – **Solution of 0.5 wt% HPAM and 0.05 wt% of chromium (III) acetate hydroxide in 75 g/L NaCl after aging for 24 hours at room temperature (a) and 40 °C (b)**

After the initial brine saturation, oil was injected into the microfluidic chip at a constant rate of 0.12 μL/min. After room-temperature oil injection overnight, the injection of oil at 40 °C reached a stabilized injection pressure of 7.3 kPa after 40 min. *Figure 6* shows photos of oil-saturated channels and the residual brine saturation. The oil appears red because it has been dyed with red oil dye.

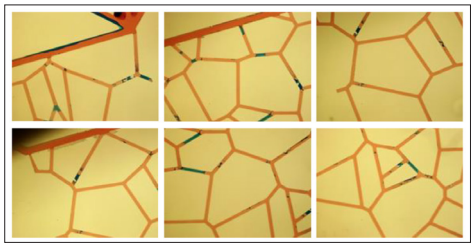

Figure 6 – **Photos of oil-saturated microchip**

In the subsequent injection of brine under the same temperature and flow rate of 0.5 and 0.12 μL/min for 150 and 135 min, respectively, the injection pressure stabilized to 1.6 kPa. Figure 7 displays photos of the channels after this brine injection, with residual oils in red.

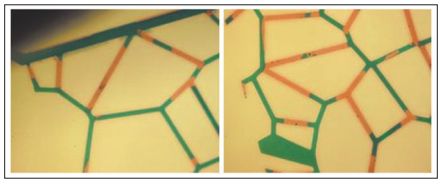

Figure 7 – **Images of microchip after brine flooding**

Then, polymer solution blended with gelling agent was injected into the microchip at room temperature. *Figure 8* illustrates the change in the injection pressure over time. It reveals that the injection pressure stabilized to 61 kPa over 150 minutes. *Figure 9* presents photos of the channels captured during injection. After this polymer injection, the microchip was aged for 24 hours at 40 °C. A comparison between *Figures 9* and *10* provides a visual distinction between fresh and matures gels in the channels.

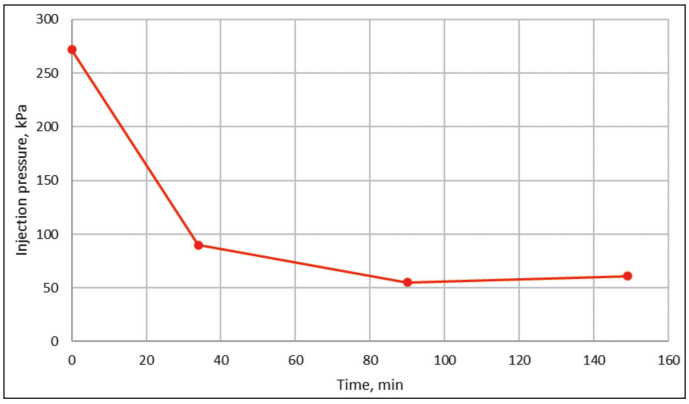

Figure 8 – **Injection pressure of the polymer solution with gelling agent: 0.5 wt% HPAM and 0.05 wt% of chromium (III) acetate hydroxide, both prepared in 75 g/L NaCl solution. Injection conditions are: 0.12 μL/min and 22.5 °C**

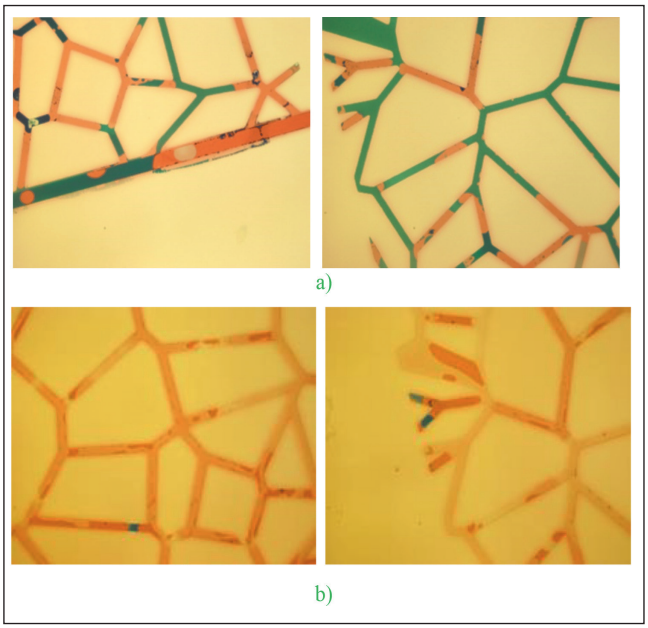

Figure 9 – **Photos of the microchip (a) before and (b) during polymer injection**

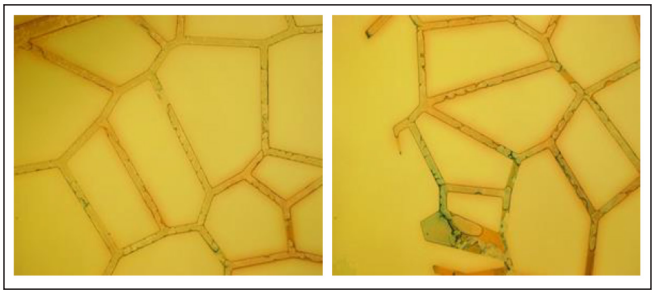

Figure 10 – **Photos of microchip after gelation**

After aging and gel formation, the model underwent a brine post-flush at a rate of 0.12 μL/min at the temperature of 40 °C. As illustrated in *Figure 11*, initial post-flush pressure was very high, 170 kPa; after nine hours of injection, post-flush pressure stabilized to 39 kPa. This implies that the permeability reduction to brine at the injection front can be as high as 100 (170/1.6) and a permeability reduction to brine after sufficient brine throughput is 24 (39/1.6). *Figure 12* shows the distribution of brine and gel inside of the channels observed during the post-flush.

In the subsequent oil injection test, conducted under the same rate and temperature conditions, the microchip developed a leak at 296 kPa (*Fig. 13*). This accident shows that the microchips fabricated using the method described in this paper may not be reliable for testing at pressures greater than 290 kPa. Nevertheless, based on data collected prior to the development of the leak, we can infer that the reduction in the permeability of oil, after gel treatment of the microchip and brine post-flush, is at least 40 (296/7.3).

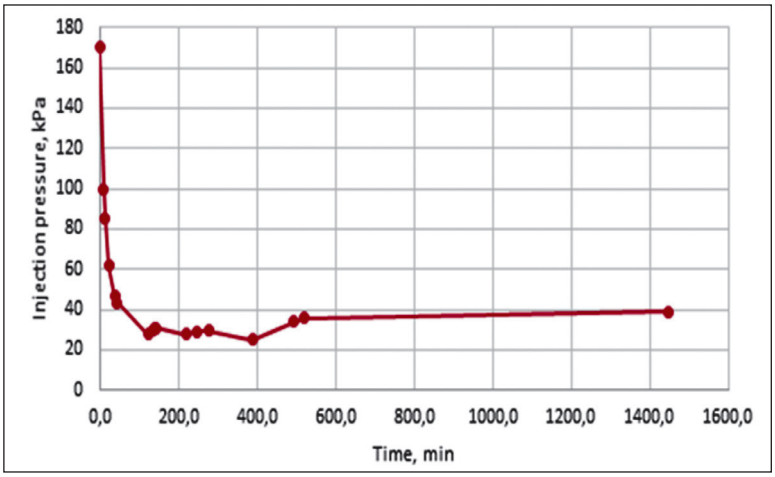

Figure 11 – **Injection pressure versus time during brine post-flush after gel treatment. Flow rate is 0.12μL/min. Temperature is 40 °C**

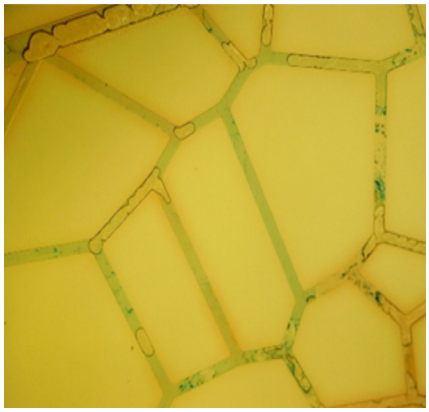

Figure 12 – **A section of the microchip 35 min after the start of post-flush (compare to Fig.10)**

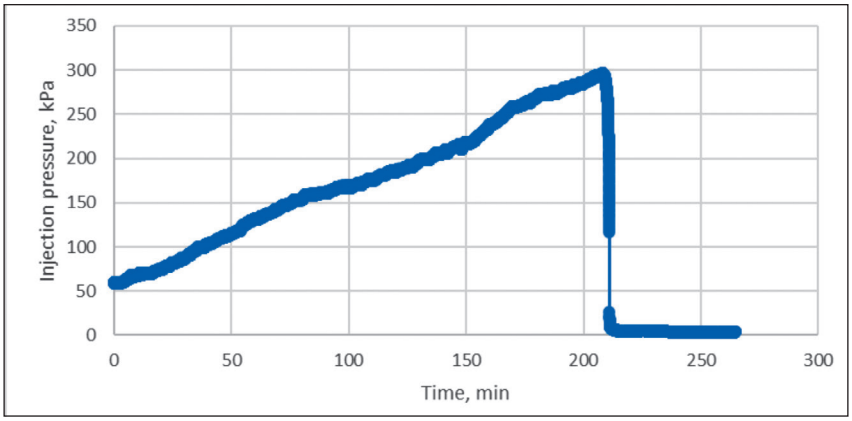

Figure 13 – **Injection pressure versus time during oil post-flush after gel treatment and brine post-flush. Flow rate is 0.12 μL/min. Temperature is 40 °C**

Table 1 summarizes the results of this study. They indicate that gels in the microchip induced a 106-fold reduction in the permeability to brine at the beginning of brine post-flush (shock front) and a 24-fold reduction after a sufficient volume of brine was injected through. At the same time there is a risk of reducing permeability to oil at least in 40 times. This indicates that a special care should be taken when injecting the gelant into production wells in order to avoid damaging oil bearing zones. We believe that the results presented here can contribute to enhancing future research methods utilizing microfluidics to study the performance and mechanisms of polymer-augmented improved/enhanced oil recovery.

Table 1 – **Measured permeability reduction of brine and oil by the very-high-molecular-weight polymer gel in NOA microchips with 50 μmwide channels**

Pre-flush		Post-flush		RRF_w		RRF_o
Oil	Brine	Brine maximal / stabilized	Oil	Maximal	Stabilized	
7.3 kPa	1.6 kPa	170 kPa / 39 kPa	More than 296 kPa	106	24	More than 40*

**Precise determination was not possible due to development of a leak in the microchip at 296 kPa.*

Conclusion

In conclusion, this study demonstrates that microfluidics a quick and cost-effective method for assessing permeability changes following the exposure of porous media to polymer gel, emphasizing the importance of integrating image-based analysis alongside pressure data in the discussion of results.

Micro-scale model experiments have revealed that the gel-polymer compound reduces oil permeability inside of microchannels of 50 μm width channels due to the obstruction of filtration channels. Specifically, the permeability of the micro-model for oil decreased by a factor of at least 40, while that for water decreased by a factor of 106 and 24 at the shock front and after sufficient throughput of brine, respectively. Taking into account these observations the injection of polymer gelant into the production well is not recommended unless the oil producing intervals are effectively isolated, otherwise a significant reduction of oil permeability can occur.

Acknowledgement

This research was possible due to the funding provided by the Committee of Science of the Ministry of Science and Higher Education of the Republic of Kazakhstan (Grant No. BR21881822 “Development of technical solutions for optimization of geological and technical operations during well drilling and oil production at the late stage of field operation”).

REFERENCES

1 Mohammad I. H., Mohammad M. K. Microfluidics: a concise review of the history, principles, design, applications, and future outlook // Biomaterials Science. – 2024. – 12(2). – P. 218-251. - https://doi.org/10.1039/D3BM01463K.

2 Zhou F., Xue-Ru C., Ya-Lan Y., Min L. Fabrication and characterization of microcapsule encapsulating EOR surfactants by microfluidic technique // Colloids and Surfaces A: Physicochemical and Engineering Aspects. – 2019. - Volume 570. – P. 282-292. - https://doi.org/10.1016/j.colsurfa.2019.02.045.

3 Ren K., Zhou J., Wu H. Materials for Microfluidic Chip Fabrication // Accounts of Chemical Research. - 2013. - 46(11) - P. 2396–2406. -DOI: 10.1021/ar300314s.

4 Niculescu, A. G., Chircov, C., Bîrcă, A. C., & Grumezescu, A. M. Fabrication and applications of microfluidic devices: A review. // International Journal of Molecular Sciences. - 2021. - V. 22. - P. 1–26. - https://doi.org/10.3390/ijms22042011.

5 Gogoi S., Gogoi S. B. Review on microfluidic studies for EOR application // Journal of Petroleum Exploration and Production Technology. - 2019. - V. 9. - P. 2263–2277. - https://doi.org/10.1007/s13202-019-0610-4.

6 Lifton, V.A. Microfluidics: an enabling screening technology for enhanced oil recovery (EOR) // The Royal Society of Chemistry. Lab on a Chip. - 2016. – 10. – P. 1777-1796. - DOI: 10.1039/c6lc00318d.

7 Fani, M., Pourafshary, P., Mostaghimi, P., Mosavat, N. Application of microfluidics in chemical enhanced oil recovery: A review // Fuel. - 2022. - Volume 315. - P. 123225. - DOI: 10.1016/j.fuel.2022.123225.

8 Saadat M., Yang J., Dudek M., Øye G., Tsai P. A. Microfluidic investigation of enhanced oil recovery: The effect of aqueous floods and network wettability // Journal of Petroleum Science and Engineering. - 2021. - V. 203. - P. 1-11. - https://doi.org/10.1016/j.petrol.2021.108647.

9 Saadat, M., Tsai, P.A., Ho, T.-H., Øye, G., & Dudek, M. Development of a Microfluidic Method to Study Enhanced Oil Recovery by Low Salinity Water Flooding // ACS Omega. - 2020. - 5(28). - P. 17521-17530. - DOI: 10.1021/acsomega.0c02005.

10 Pryazhnikov M.I., Minakov A.V., Pryazhnikov A.I., Denisov I.A.,YakimovA.S. Microfluidic Study of the Effect of Nanosuspensions on Enhanced Oil Recovery // Nanomaterials. - 2022. - 12(3). - P. 1-15. - https://doi.org/10.3390/nano12030520.

11 Liang B., Jiang H., Li J., Seright R. S., Lake L. W.Further Insights into the Mechanism of Disproportionate Permeability Reduction //Paper presented at the SPE Annual Technical Conference and Exhibition - San Antonio, Texas, USA, October 2017. - P. 1-19. https://doi.org/10.2118/187364-MS.